TWO YEARS OF GLOBAL CIRRUS CLOUD STATISTICS USING HIRS

Donald Wylie
CIMSS
University of Wisconsin-Madison

and

W. Paul Menzel
Satellite Applications Laboratory
NOAA/NESDIS
Madison, Wisconsin 53706

ABSTRACT

A climatology of upper tropospheric semi-transparent cirrus clouds has been compiled using HIRS multispectral infrared data sensitive to CO_2 absorption from the NOAA polar orbiting satellites. This is a report on the first two years of data analyzed (June 1989 - May 1991). Semi-transparent clouds were found in 36% of the observations. Large seasonal changes were found in these clouds in many geographical areas; large changes occur in areas dominated by the ITCZ, the sub-tropical high pressure systems, and the mid-latitude storm belts. Semi-transparent clouds associated with these features, move latitudinally with the seasons. These clouds also are more frequent in the summer hemisphere than the winter hemisphere. They appear to be linked to convective cloud development and the mid-latitudinal frontal weather systems.

INTRODUCTION

Clouds have long been recognized as playing a major role in modulating the radiation budget in the earth's climate system. Attempts to characterize the frequency of cloud occurrence and associated cloud properties have relied heavily on inferences made from satellite radiance observations. Without satellite data, little is known about clouds over oceans and sparsely populated regions of the globe because ground based weather observations are concentrated only in the populated areas. Cirrus clouds are crucially important to global radiative processes and the heat balance of the Earth; they allow solar heating while reducing infrared radiation to space. Models of climate changes will have to correctly simulate these clouds to have the proper radiative terms for the Earth's heat budget.

Past estimates of the variation of cloud cover and the earth's outgoing longwave radiation have been derived primarily from the longwave infrared window (10-12 microns) radiances observed from polar orbiting and geostationary satellites (Rossow and Lacis, 1990; Gruber and Chen, 1988). The occurrence of semi-transparent clouds is often underestimated in these single channel approaches. Recently, multispectral techniques have been used to better detect cirrus in global (Wu and Susskind, 1990) and North American (Wylie and Menzel, 1989) cloud studies.

This paper reports on the investigation of seasonal changes in the cirrus or semi-transparent global cloud cover with two years of multispectral observations from the polar orbiting HIRS (High resolution Infrared Radiation Sounder). Transmissive clouds that are partially transparent to terrestrial

radiation have been separated from opaque clouds in the statistics of cloud cover (Wylie and Menzel, 1989). Semi-transparent or cirrus clouds are found in roughly 30 to 35% of all satellite observations.

The HIRS observations in the carbon dioxide absorption band at 15 microns have been used to calculate these cloud statistics. The CO_2 slicing algorithm calculates both cloud top pressure and effective emissivity from radiative transfer principles. Various CO_2 algorithms have been described in the literature (Chahine, 1974; Smith et al., 1974; Smith and Platt, 1978; Menzel et al., 1983) and applications to data from the geostationary sounder VAS (VISSR Atmospheric Sounder) and the polar orbiting sounder HIRS have been published (Wylie and Menzel, 1989; Menzel et al., 1986; Susskind et al., 1987; Menzel et al., 1989, Eyre and Menzel, 1989). The technique has been described in previous articles (Menzel et al., 1989) and will only be briefly summarized here.

TECHNIQUE

Cirrus clouds often appear warmer in the window channel than the ambient air temperature at their altitude because they are transmitting radiation from below. This occurs in approximately 40% of the satellite data. The "CO_2 Slicing" technique is capable of detecting these clouds using the HIRS infrared channels with partial CO_2 absorption. It has the ability to distinguish partially transmissive clouds both during daylight and at night and over either water or land backgrounds. The technique is described in Menzel et al. (1989) and is repeated in Appendix A of this paper. A cloud top pressure and effective emissivity are calculated for a given observational area.

Effective emissivity refers to the product of the fractional cloud cover, N, and the cloud emissivity, ϵ, for each observational area (roughly 30 km by 30 km). When $N\epsilon$ is less than unity, HIRS may be observing broken opaque cloud ($N<1$, $\epsilon=1$), overcast transmissive cloud ($N=1$, $\epsilon<1$), or broken transmissive cloud ($N<1$, $\epsilon<1$). All of these possibilities are labelled as "cirrus" in this paper. It is not possible to distinguish amongst them with the CO_2 slicing technique. Here, "cirrus" refers to an observation where the HIRS radiometer detects radiation from below a cloud layer as well as radiation from the cloud layer top. Effective emissivity observations less than 0.95 are labelled as cirrus while those greater than 0.95 are considered to be opaque clouds.

The technique is limited to finding the height of only the highest cloud layer in a multiple cloud layered situation. Cloud base altitude cannot be measured. Multiple layers often can be inferred from inspection of neighboring pixels where holes in the upper layer occur. Comparison to cloud reports from ground observers indicate that 50% of the time when the CO_2 technique detects an upper tropospheric cloud, one or more lower cloud layers also is present. Appendix B discusses the problems of the CO_2 slicing technique in multilayer cloud situations. For multilayer cloud situations where an opaque cloud underlies a transmissive cloud, the errors in the height of the transmissive cloud are about 100 mb too low in the atmosphere for most cases. The error is largest when the underlying opaque layer is in the middle troposphere (400-700 mb) and smallest when the opaque cloud is near the surface or close to the transmissive layer. The error in effective emissivity

increases as the opaque layer approaches the transmissive layer; when they are coincident the effective emissivity is set to one.

GLOBAL CLOUD STATISTICS

A statistical summary of all the cloud observations made from June 1989 through May 1991 is shown in Table 1. Over 6 million observations were processed. The cloud top pressure determinations were subdivided into ten vertical levels from 100 mb to 1000 mb and effective emissivities were subdivided into five intervals from 0 to 1.00.

Table 1 reveals that high clouds above 400 mb comprised 20% of the observations. 30% of the observations were of clouds between 400 mb and 700 mb. Low clouds below 700 mb were found 22% of the time. Clear sky conditions were found 28% of the time.

Cirrus clouds (observations with effective emissivities less than 0.95) were found in 36% of our observations; they ranged from 100 to 700 mb. Clouds opaque to infrared radiation (observations with effective emissivities greater than 0.95) were found 36% of the time.

As the satellite views from above the atmosphere, high clouds were found in preference to low clouds. Broken low cloud fields were reported as opaque low clouds because of the technique's inability to sense the cloud fraction below the peaks in the CO_2 channels, as previously mentioned. The transmissive clouds covered the range of effective emissivities from 0.0 to 0.95 fairly uniformly. Approximately 9% were found in each category.

As discussed in Menzel and Wylie (1991), the CO_2 slicing technique is subject to some errors. The large observation area (30 km by 30 km) produces results where the semi-transparent cloud observations are overestimated by roughly 5%. The HIRS lack of sensitivity to very thin clouds causes roughly 5% of the semi-transparent clouds to be incorrectly classified (Wylie and Menzel, 1989). Fortunately, these large errors are offsetting. Overall, because of the very large sample size and the relative accuracy of the CO_2 slicing technique, we claim that the entries in Table 1 are valid within 1%; all values should be interpreted as +/-0.5%.

SEASONAL AND GEOGRAPHICAL TRENDS

Figure 1 shows the winter and summer (referenced to the northern hemisphere) distribution of all clouds over land and ocean as a function of latitude. Over the oceans a rather uniform cloudiness is observed from 60 N to 60 S; over land there is a equatorial peak that follows the sun.

A large seasonal change was found over Antarctica, where few clouds of any altitude were reported in the northern summer (southern winter). The HIRS data do not show polar stratospheric clouds, which occur commonly over Antarctica in the southern winter. Polar stratospheric clouds apparently do not attenuate the HIRS channels sufficiently to mask out the strong inversions below them. In the Antarctic, the HIRS 700 mb channel is often warmer than the window channel indicating that the air temperature around 700 mb is warmer than the surface. It has been assumed that the inversions seen by HIRS indicated radiative cooling under clear skies, therefore these observations

were classified as cloud free. When no inversion is apparent (the 700 mb channel reported temperatures within 2 K of the window channel), it has been assumed that both channels saw the top of a cloud and the observation was classified as cloudy.

The remaining discussion will concentrate on the upper tropospheric clouds (above 500 mb). This includes both the transmissive and opaque clouds, which were 32% and 5% of all observations respectively. Figure 2 shows the zonal distribution of high clouds where the cloudiness in the Inter-Tropical Convergence Zone (ITCZ) is prominent. Secondary maxima in high cloud frequency are found in the mid-latitude storm belts. Seasonal shifts in the ITCZ are apparent both over land and ocean, the ITCZ moving north and south with the sun. High clouds increase strongly from the equator to 30 S during the northern hemispheric winter which is the southern summer.

Figure 3 shows the geographical distribution of transmissive clouds in summer and winter (darker regions indicate less frequent cloud occurrence). Large convective development occurs during the winter (southern summer) in South America and Africa which is readily apparent through increased occurrence of transmissive clouds. This explains the high cloud cover change in the winter from the equator to 30 S.

Over the oceans, the ITCZ is most apparent in the northern summer. Figure 2 indicates that high clouds were more frequent from the equator to 10 N in this season. During the southern summer, the ITCZ moved south of the equator and covered more latitude than in the northern winter. This is most apparent in the western Pacific (Fig. 3) where a southern extension of the ITCZ was present.

The seasonal movement of the sub-tropical high pressure systems also is apparent in both hemispheres as the cloud minima around 20 - 30 latitude moves with the ITCZ. High clouds were less (more) frequent in the winter (summer) season in both hemispheres; A similar seasonal change also occurred in the sub-tropical deserts at 10 - 25 N and 10 - 35 S (Fig. 2).

The northern hemispheric land masses from 45 to 75 N latitude show little seasonal change in high cloud cover (Fig. 2). This seasonal consistency of semi-transparent clouds agrees with the GOES/VAS analysis over the continental U.S. (Wylie and Menzel, 1989).

The southern hemispheric storm belt over ocean, 30 - 60 S, exhibited regional seasonal changes in high cloud frequency, especially in the south Atlantic and south Indian Oceans (Fig. 3). However when averaged latitudinally, the increase is less apparent (Fig. 2).

In the northern hemisphere mid-latitude storm belts, 30 - 50 N, large seasonal change in high cloud cover were evident in both oceans (Fig. 2). The frequency of high clouds increased during the northern winter with the strengthening of the Alleutian Low in the north Pacific and the Icelandic Low in the north Atlantic. The cloud cover from both lows can be readily seen in the geographical plot (Fig. 3).

Figure 4 shows the latitudinal distribution of thin transmissive (Nε less than .5) clouds for all seasons. The occurrence is slightly more likely

over the ocean, and a modest peak from the equator to 10 N is evident both over land and ocean. Thin transmissive clouds appear globally with a frequency of 20 to 40%.

CONCLUSIONS

There is a global preponderance of semi-transparent high clouds, presumed to be cirrus; 36% on the average for the last two years. In the ITCZ a high frequency of cirrus (greater than 50%) is found at all times; a modest seasonal movement tracks the sun. Large seasonal changes in cloud cover occur over the oceans in the storm belts at midlatitudes; the concentrations of these clouds migrated north and south with the seasons following the movement of convective systems (more cirrus is found in the summer than in the winter in each hemisphere). At higher latitudes cirrus were located with the cyclonic storms and frontal systems. At even higher latitudes, between 45 - 75, little seasonal change in cirrus is found. Over North America, cirrus show little seasonal chnage as they are found in regions of weak dynamics as well as strong.

APPENDIX A. TECHNIQUE DESCRIPTION

The HIRS radiometer senses infrared radiation in eighteen spectral bands that lie between 3.9 and 15 microns at 25 to 40 km resolution (depending upon viewing angle) in addition to visible reflections at the same resolution. The four channels in the CO_2 absorption band at 15 microns are used to differentiate cloud altitudes and the longwave infrared window channel identifies the effective emissivity of the cloud in the HIRS field of view (FOV).

To assign a cloud top pressure to a given cloud element, the ratio of the deviations in cloud produced radiances, $R_{cld}I(\nu)$, and the corresponding clear air radiances, $R_{clr}(\nu)$, for two spectral channels of frequency ν_1 and ν_2 viewing the same FOV can be written as

$$\frac{R_{cld}(\nu_1) - R_{clr}(\nu_1)}{R_{cld}(\nu_2) - R_{clr}(\nu_2)} = \frac{\epsilon_1 \int_{P_s}^{P_c} \tau(\nu_1,p) \frac{dB[\nu_1, T(p)]}{dp} dp}{\epsilon_2 \int_{P_s}^{P_c} \tau(\nu_2,p) \frac{dB[\nu_2, T(p)]}{dp} dp} . \quad (1)$$

In this equation, ϵ is the cloud emissivity, P_s the surface pressure, P_c the cloud pressure, $\tau(\nu,p)$ the fractional transmittance of radiation of frequency ν emitted from the atmospheric pressure level (p) arriving at the top of the atmosphere (p = 0), and $B[\nu,T(p)]$ is the Planck radiance of frequency ν for temperature T(p). If the frequencies are close enough together, then ϵ_1 approximates ϵ_2, and one has an expression by which the pressure of the cloud within the FOV can be specified.

The left side of Eq. (1) is determined from the satellite observed radiances in a given fov and the clear air radiances inferred from spatial analyses of satellite clear radiance observations. The right side of Eq. (1)

is calculated from a temperature profile and the profiles of atmospheric transmittance for the spectral channels as a function of P_c, the cloud top pressure (1000 mb to 100 mb is spanned by discrete values at 50 mb intervals). In this study, global analyses of temperature and moisture fields from the National Meteorological Center (NMC) are used. The P_c that best matches observed and calculated ratios is the desired solution.

Once a cloud height has been determined, an effective cloud amount (also referred to as effective emissivity in this paper) can be evaluated from the infrared window channel data using the relation

$$N\epsilon = \frac{R_{cld}(w) - R_{clr}(w)}{B[w, T(P_c)] - R_{clr}(w)} . \qquad (2)$$

Here N is the fractional cloud cover within the FOV, $N\epsilon$ the effective cloud amount, w represents the window channel frequency, and $B[w, T(P_c)]$ is the opaque cloud radiance.

Using the ratios of radiances of the three CO_2 spectral channels, four separate cloud top pressures can be determined (14.2/14.0, 14.0/13.7, 14.0/13.3, and 13.7/13.3). Whenever (R_{cld}-R_{clr}) is within the noise response of the instrument (roughly 1 mW/m2/ster/cm-1), the resulting P_c is rejected. Using the infrared window and the four cloud top pressures, as many as four effective cloud amount determinations can also be made. As described by Menzel (1983), the most representative cloud height and amount are those that best satisfy the radiative transfer equation for the four CO_2 channels.

If no ratio of radiances can be reliably calculated because (R_{cld}-R_{clr}) is within the instrument noise level, then a cloud top pressure is calculated directly from the comparison of the HIRS observed 11.2 micron infrared window channel brightness temperature with an in situ temperature profile and the effective emissivity is assumed to be unity. In this way, all clouds are assigned a cloud top pressure either by CO_2 or infrared window calculations.

Fields of view are determined to be clear or cloudy through inspection of the 11.2 micron brightness temperature with an 8.3 micron channel correction for moisture absorption. If the moisture corrected 11.2 micron brightness temperature is within 2 degrees Kelvin of the known surface temperature (over land this is inferred from the 1000 mb NMC model analysis adjusted with observations from the Global Telecommunications System surface network; over the oceans this is the NMC sea surface temperature), then the FOV is assumed to be clear (P_c = 1000 mb) and no cloud parameters are calculated.

The HIRS data from NOAA 10 and 11 were sampled to make the processing more manageable. Only every third pixel on every third line were used. The data also were edited for zenith scan angles, eliminating data over 10^o to minimize any problems caused by the increased path length through the atmosphere of radiation upwelling to the satellite. It restricted the coverage to approximately the center one third of the orbit swath. With two satellites, about one half of the Earth is sampled each day.

APPENDIX B. ERRORS ASSOCIATED WITH THE PRESENCE OF A LOWER CLOUD LAYER

The algorithm assumes that there is only one cloud layer. However, for over 50% of satellite reports of upper tropospheric opaque cloud, the ground observer indicates additional cloud layers below. To understand the effects of lower cloud layers, consider the radiation sensed in a cloudy field of view. For a semi-transparent or cirrus cloud layer, the radiation reaching the satellite, R_{cld}, is given by

$$R_{cld} = R_a + \epsilon * R_c + (1-\epsilon) * R_b \qquad (3)$$

where R_a is the radiation coming from above the cloud, R_c is the radiation coming from the cloud itself, R_b is the radiation coming from below the cloud, and ϵ is the cloud emissivity. When a lower cloud layer is present under the semi-transparent or cirrus cloud, R_b is smaller (i.e., some of the warmer surface is obscured by the colder cloud). If prime indicates a two layer cloud situation of high semi-transparent cloud over lower cloud, and no prime indicates the single layer high semi-transparent cloud, then

$$R_b' < R_b, \qquad (4)$$

which implies

$$R_{cld}' < R_{cld}. \qquad (5)$$

Thus the difference of cloud and clear radiance is greater for the two layer situation,

$$[R_{clr} - R_{cld}'] > [R_{clr} - R_{cld}] \; . \qquad (6)$$

The effect of two cloud layers is greater for the 13.3 micron channel than for the other CO_2 micron channels, because the 13.3 micron channel "sees" lower into the atmosphere (it has a non zero transmittance from low in the atmosphere). So using the 14.0/13.3 ratio as an example

$$[R_{clr}(13.3) - R_{cld}'(13.3)] > [R_{clr}(14.0) - R_{cld}'(14,0)]. \qquad (7)$$

This reduces the ratio of the clear minus cloud radiance deviation in Eq. (1) because the denominator is affected more than the numerator (when the less transmissive channel is in the numerator),

$$\frac{[R_{clr}(14.0) - R_{cld}'(14.0)]}{[R_{clr}(13.3) - R_{cld}'(13.3)]} < \frac{[R_{clr}(14.0) - R_{cld}(14.0)]}{[R_{clr}(13.3) - R_{cld}(13.3)]} \; , \qquad (8)$$

or $L1' < L1$, where L1 refers to the left side of Eq. (1). An example plot of P_c versus R1 (where R1 refers to the right side of Eq. (1)), shown in Figure 5, indicates that $L1' < L1$ implies $P_c' > P_c$. Thus, when calculating a cloud pressure for the upper semi-transparent cloud layer in a two cloud layer situation, the CO_2 slicing algorithm places the upper cloud layer too low in the atmosphere.

An example from 25 April 1991 is presented to illustrate further the magnitude of the errors that can be induced by lower level clouds (results for other days and other situations were found to be comparable). Observers in the Kwajalein Islands reported high cirrus clouds with no other underlying clouds present. The ratio of the 14.0 to 13.3 micron satellite observed radiance differences between clear and cloudy FOVs (the left side of Eq. (1)) is 0.41 on 25 April. This implies single layer cloud at 300 mb (solving the right side of Eq. (1) for P_c as shown in Fig. 5).

As explained above, if there had been an opaque cloud layer below 300 mb, R_{cld}' would have been smaller than measured for these cases. The changes in R_{cld}' were modelled for underlying opaque cloud layers at 850, 700, 600, 500, 400 and 300 mb (producing different ratios L1' in the left side of Eq. (1)). These changes will suggest different P_c' solutions as R1, the right side of Eq. (1), is matched to L1'. In the absence of any knowledge of a lower layer, the CO_2 algorithm integrates the right side of Eq. (1) from the surface to an incorrect P_c'. Figure 5 shows R1 as a function of P_c for the situation of 25 April. The errors in calculated cloud top pressure from the original 300 mb solution, $P_c' - P_c$, are shown as a function of height of the underlying opaque cloud layer in Figure 6 for 25 April.

In the two cloud layer situation, the position of the lower cloud layer affects the accuracy of the estimate of the height of the upper cloud layer. Opaque clouds in the lower troposphere near the surface underneath high cirrus have little affect on the cirrus P_c. The 14.2, 14.0, and 13.7 micron channels are not sensitive to radiation from low in the troposphere, but the 13.3 micron channel senses about one third of the radiation from below 800 mb. Opaque clouds in the middle troposphere, between 400 and 800 mb, underneath high cirrus, cause the cirrus P_c to be overestimated (lower in the atmosphere) by up to 190 mb (this extreme occurs for the very thin high cirrus cloud with $N\epsilon$ of .10). The decreases in R_b produce smaller ratios for the left side of (1) which in turn produces larger estimates of P_c. Opaque clouds high in the atmosphere, underneath higher cirrus, have little effect on the cirrus P_c, since the height of the lower opaque layer approaches the height of the semi-transparent upper cloud layer and the CO_2 algorithm is going to estimate a height in between the two layers.

The errors in P_c were also examined for different emissivities of transmissive clouds (see Fig. 6). This was modelled by varying the emissivity in Eq. (3) and forming new ratios on the left side of Eq. (1). The maximum cloud top pressure error of roughly 190 mb occurred in very thin cloud with emissivity of .10. The error in P_c reduced as the emissivity of the transmissive clouds increased. For a cloud with emissivity of 0.5, the maximum error in P_c is about 60 mb. For more dense clouds with emissivity of 0.9, the maximum error in P_c is less than 10 mb. The satellite cloud data have shown a nearly uniform population of emissivity center around 0.5 (Wylie and Menzel, 1989), so one can conclude that the errors in the cloud top pressure caused by underlying clouds should average under 100 mb.

Multi-layer cloud situations (transmissive over opaque cloud) cause the height estimate of the upper cloud to be about 100 mb too low in the atmosphere on the average. The error in transmissive cloud height is largest when the underlying opaque layer is in the middle troposphere (400- 700 mb) and small to negligible when the opaque layer is near the surface or close to

the transmissive layer. The error in effective emissivity increases as the opaque layer approaches the transmissive layer; when they are coincident the effective emissivity is assumed to be one. These errors due to multi-layer clouds suggest that overall these HIRS estimates may be putting global clouds a little low in the atmosphere and with an effective emissivity a little too high.

REFERENCES

Chahine, M. T., 1974: Remote sounding of cloudy atmospheres. I. The single cloud layer. J. Atmos. Sci., 31, 233-243.

Eyre, J. R., and W. P. Menzel, 1989: Retrieval of cloud parameters from satellite sounder data: A simulation study. J. Appl. Meteor., 28, 267-275.

Gruber, A., and T. S. Chen, 1988: Diurnal variation of outgoing longwave radiation. J. Clim. Appl. Meteor., 8, 1-16.

Menzel, W. P., W. L. Smith, and T. R. Stewart, 1983: Improved cloud motion wind vector and altitude assignment using VAS. J. Clim. Appl. Meteor., 22, 377-384.

Menzel, W. P., D. P. Wylie, and A. H.-L. Huang, 1986: Cloud top pressures and amounts using HIRS CO_2 channel radiances. Technical Proceedings of the Third International TOVS Study Conference, 13-19 August 1986, Madison, WI, 173-185.

Menzel, W. P., D. P. Wylie, and K. I. Strabala, 1989: Characteristics of global cloud cover derived from multispectral HIRS observations. Technical Proceedings of the Fifth International TOVS Study Conference, 24-28 July 1989, Toulouse, France, 276-290.

Menzel, W. P., Wylie, D. P., and Strabala, K. I., 1991: Seasonal and diurnal changes in cirrus clouds as seen in four years of observations with the VAS. Submitted to. J. of Appl. Meteor.

Rossow, W. B., and A. A. Lacis, 1990: Global and seasonal cloud variations from satellite radiance measurements. Part II: Cloud properties and radiative effects. J. Clim., in press.

Shapiro, M. A., and P. J. Kennedy, 1981: Research aircraft measurements of jet stream geostrophic and ageostrophic winds. J. Atmos. Sci., 38, 2642-2652.

Smith, W. L., H. M. Woolf, P. G. Abel, C. M. Hayden, M. Chalfant, and N. Grody, 1974: Nimbus 5 sounder data processing system. Part I: Measurement characteristics and data reduction procedures. NOAA Tech. Memo. NESS 57, 99pp.

Smith, W. L., and C. M. R. Platt, 1978: Intercomparison of radiosonde, ground based laser, and satellite deduced cloud heights. J. Appl. Meteor., 17, 1796-1802.

Susskind, J., D. Reuter, and M. T. Chahine, 1987: Cloud fields retrieved from analysis of HIRS/MSU sounding data. J. Geophys. Res., 92, 4035-4050.

Wielicki, B. A., and J. A. Coakley, 1981: Cloud retrieval using infrared sounder data: Error analysis. J. Appl. Meteor., 20, 157-169.

Wu, M. L. and J. Susskind, 1990: Outgoing longwave radiation computed from HIRS2/MSU soundings. J. Geophys. Res., 95D, 7579-7602.

Wylie, D. P., C. Grund, and E. Eloranta, 1989: Seasonal and diurnal changes in cloud obscurations to visible and infrared energy transmission. Proc. SPIE, 1060, 201-208.

Wylie, D. P., and W. P. Menzel, 1989: Two years of cloud cover statistics using VAS. J. Clim. Appl. Meteor., 2, 380-392.

Table 1: HIRS two year global cloud statistics (June 1989 to May 1991). The frequency of cloud observations for different heights and effective emissivities. Percentages are of the total number of observations, clear and cloudy combined. Clouds were not detected in 28% of the observations.

	ALL CLOUDS	EFFECTIVE EMISSIVITY				
LEVEL		<0.25	<0.50	<0.75	<0.95	>0.95
<200 mb	4%	1%	1%	0%	1%	1%
<300 mb	7	2	1	1	1	2
<400 mb	9	2	2	2	2	1
<500 mb	11	2	2	3	2	2
<600 mb	10	1	2	3	1	3
<700 mb	9	0	1	2	1	5
<800 mb	7	0	0	0	0	7
<900 mb	9	0	0	0	0	9
<1000 mb	6	0	0	0	0	6
Total	72%	8%	9%	11%	8%	36%

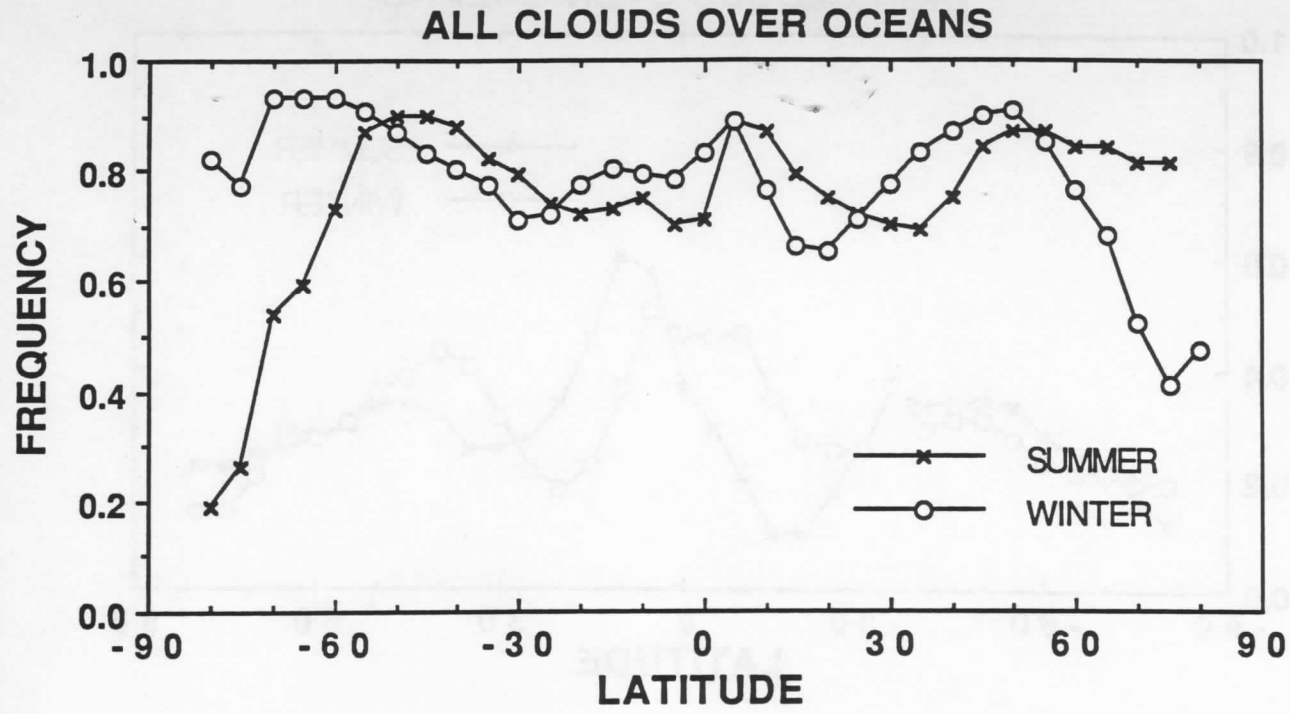

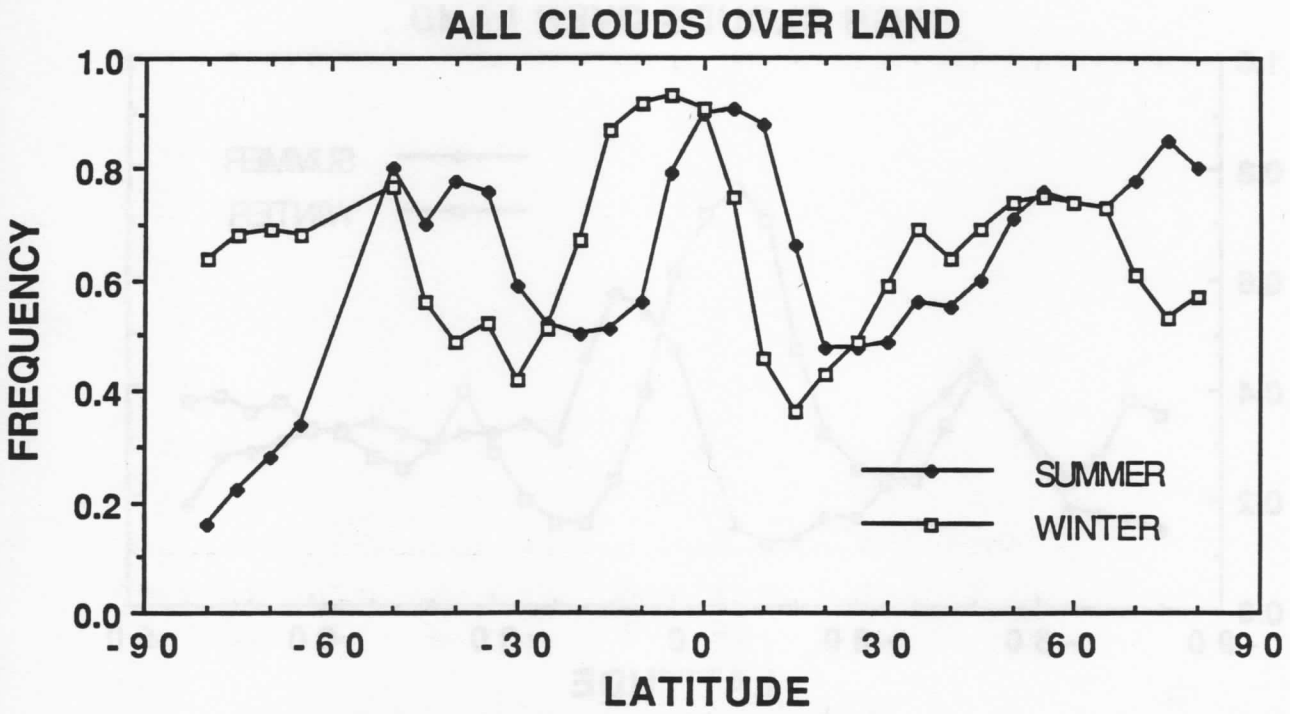

Figure 1: (a) The frequency of all clouds over ocean as a function of latitude for the summers of 1989-90 and winters 89-90 (northern hemisphere) expressed as a fraction of all satellite observations, clear and cloudy combined. (b) The same over land.

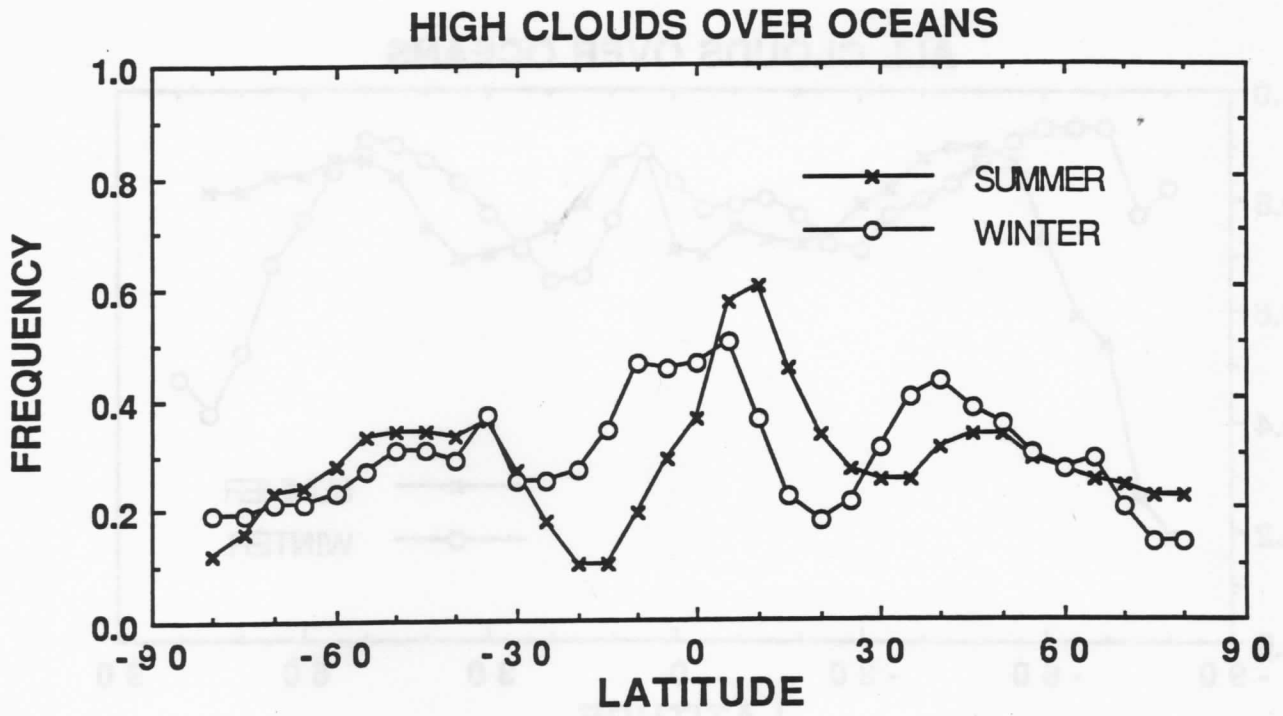

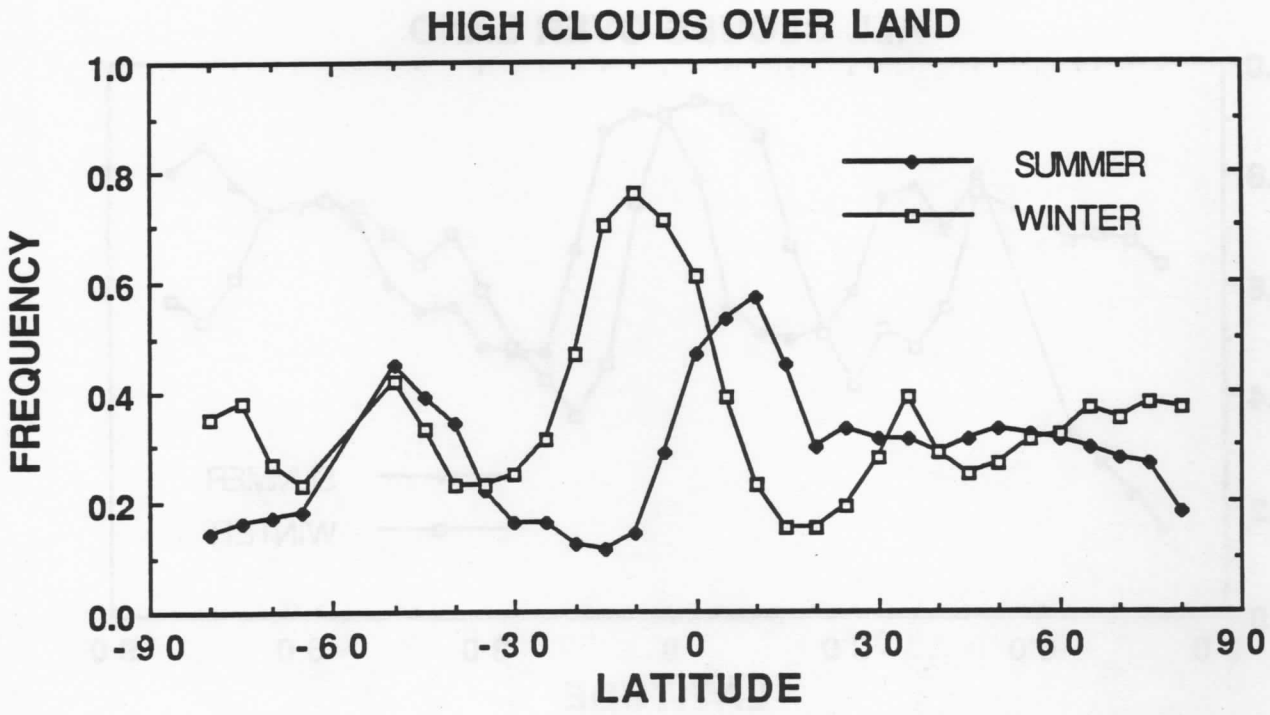

Figure 2: (a) The frequency of high clouds, <500 mb, over ocean as a function of latitude for the summers of 1989-90 and winters 89-90 (northern hemisphere) expressed as a fraction of all satellite observations, clear and cloudy combined. (b) The same over land.

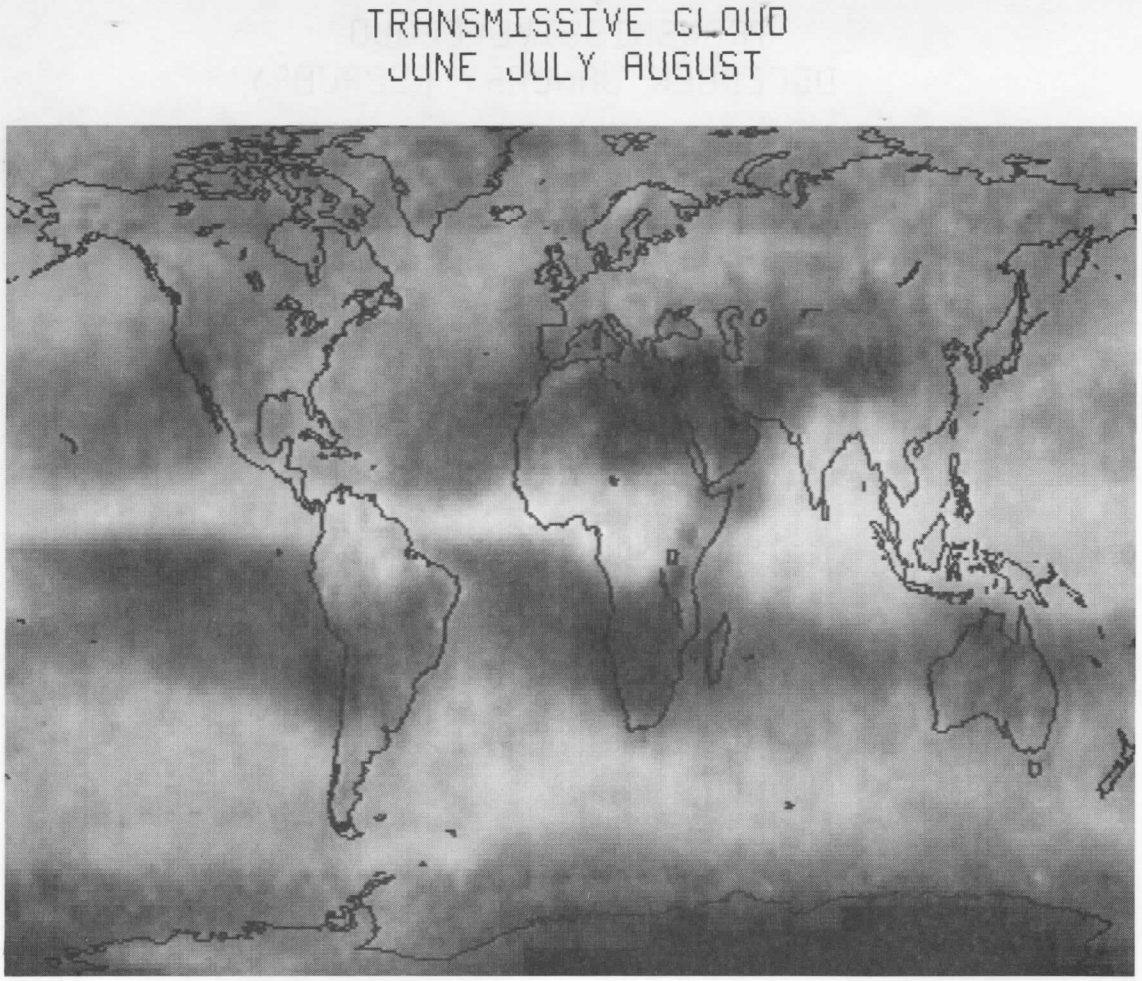

Figure 3: (a) The geographic frequency of transmissive clouds for the summers (June, July, August) during the observation period June 1989 to May 1991.

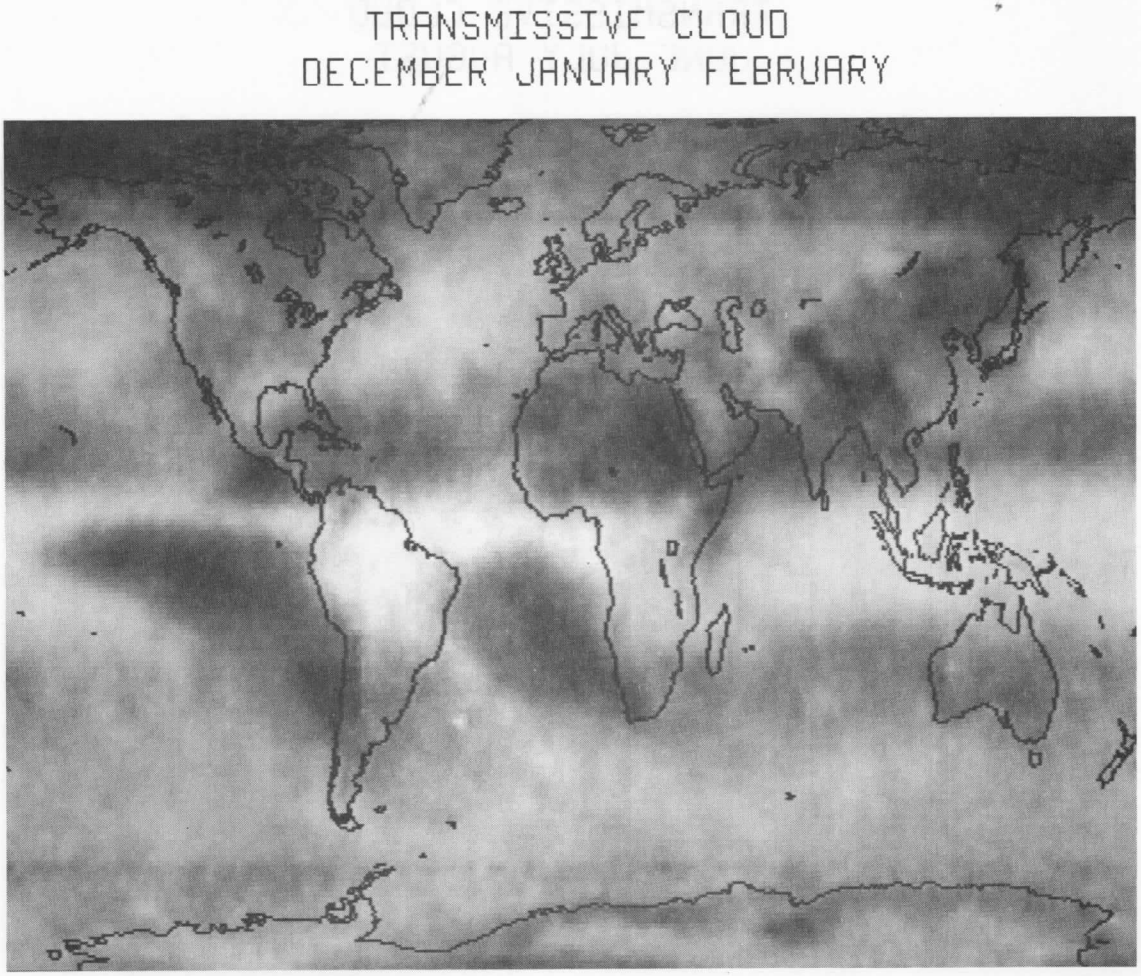

Figure 3: (b) The geographic frequency of transmissive clouds for the winters (December, January, and February) during the observation period June 1989 to May 1991.

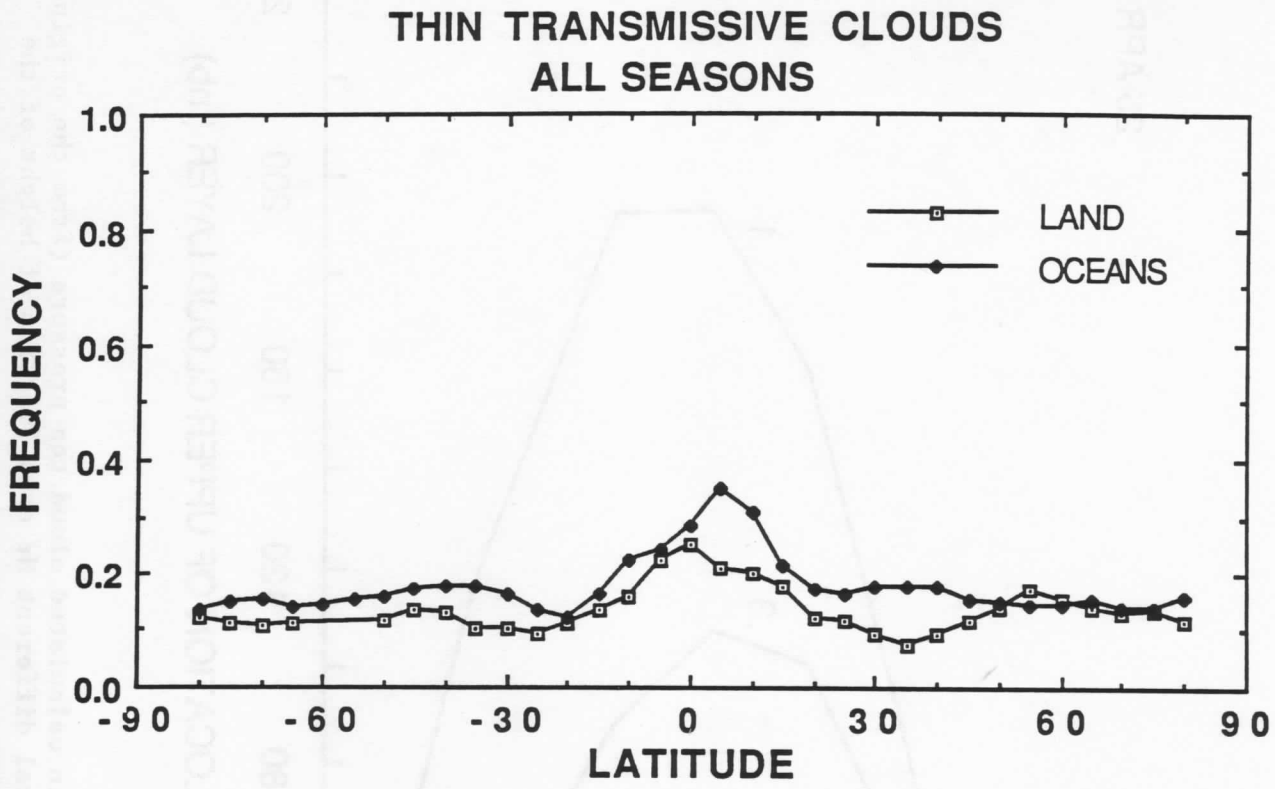

Figure 4: The frequency of thin transmissive (Nε less than .5) over ocean and land as a function of latitude for the observation period June 1989 to May 1991 expressed as a fraction of all satellite observations, clear and cloudy combined.

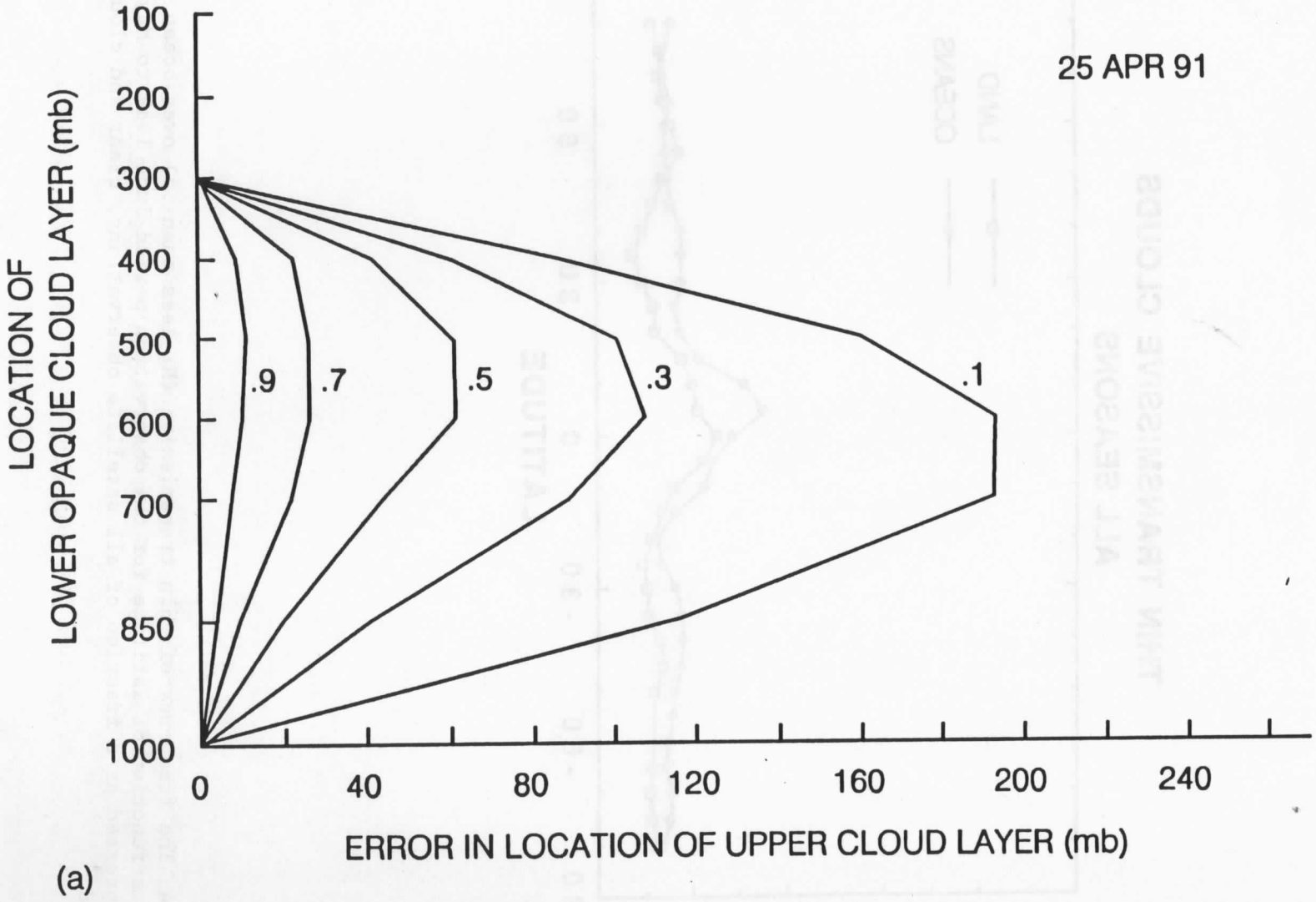

Figure 6: (a) The errors in calculated cloud top pressure (from the original 300 mb solution) for several different Nε as a function of height of the underlying opaque cloud layer.

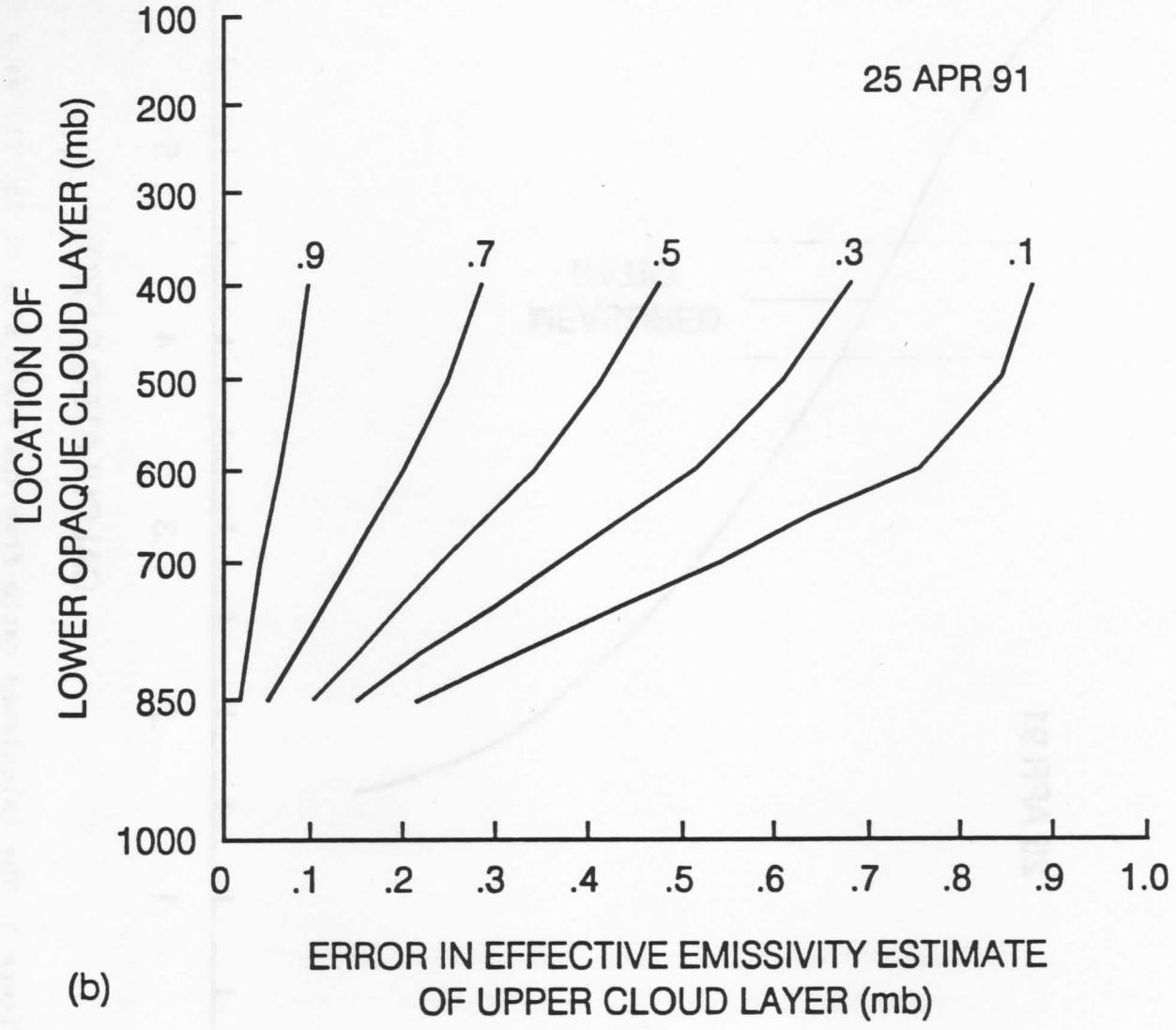

Figure 6: (b) The errors in effective emissivity (from the original solution of $N\epsilon$) as a function of height of the underlying opaque cloud layer.

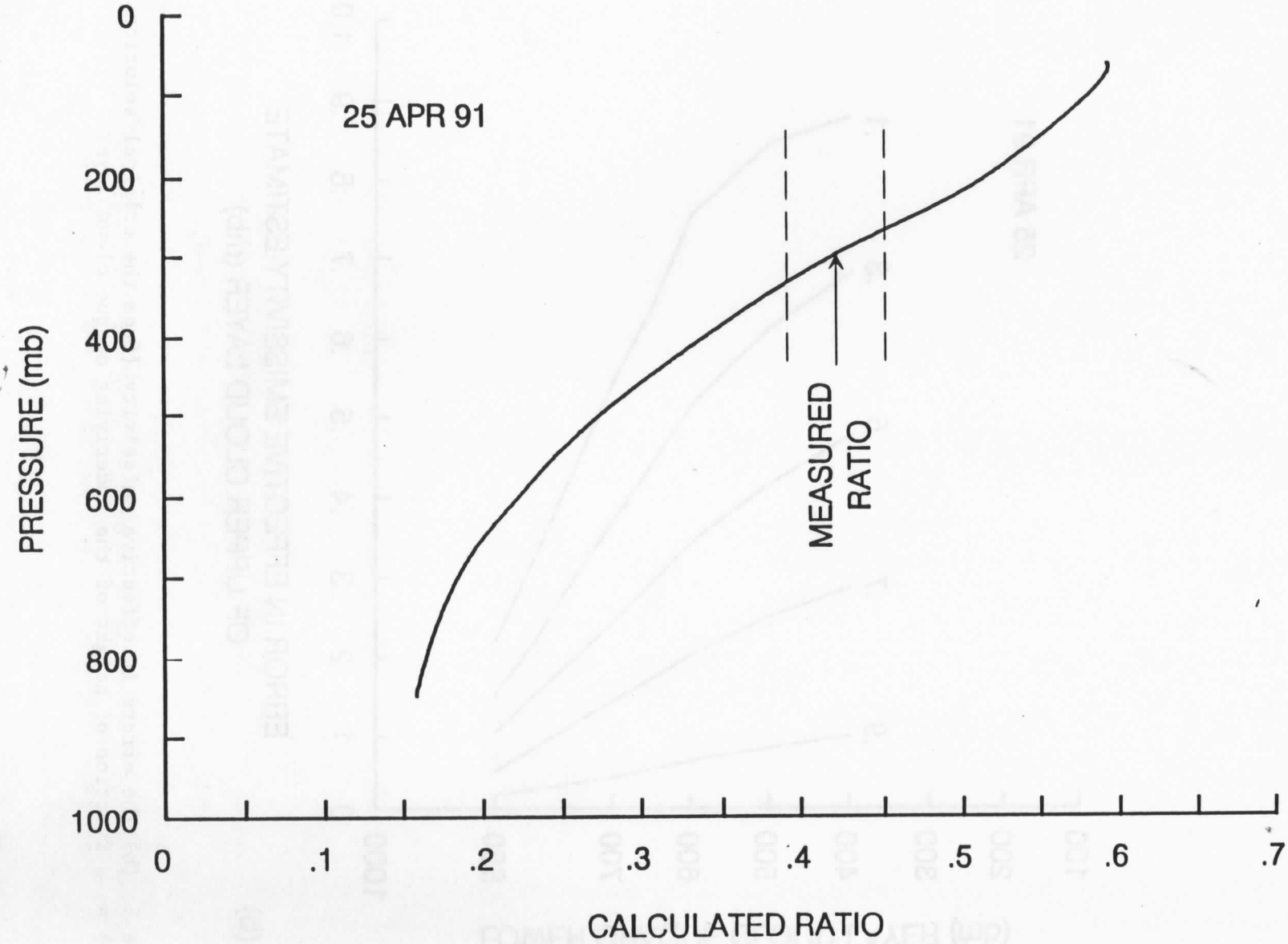

Figure 5: The calculated ratio from the right side of Eq. (1) as a function of cloud top pressure for the sounding of 25 April 1991 at the Kwajalein Island. The measured ratio from the left side of Eq. (1) is indicated. The cloud top pressure is inferred to be 300 mb.

TECHNICAL PROCEEDINGS OF THE SIXTH INTERNATIONAL TOVS STUDY CONFERENCE

AIRLIE, VIRGINIA

1-6 MAY 1991

Edited by

W. P. Menzel

Cooperative Institute for Meteorlogical Satellite Studies
Space Scienceand Engineering Center
University of Wisconsin
1225 West Dayton Street
Madison, Wisconsin

July 1991